SMAR 2015 – Third Conference on Smart Monitoring,
Assessment and Rehabilitation of Civil Structures

SMAR 2015

# Structural Performance of Superelastic SMA Reinforced Concrete Beam Subjected to Cyclic Loading

M.Ajmal[1], M.K.Rahman[2], and M.H.Baluch[1]

[1] Department of Civil Engineering, King Fahd University of Petroleum & Minerals (KFUPM), Dhahran, Saudi Arabia
[2] Center for Engineering Research, Research Institute, King Fahd University of Petroleum & Minerals (KFUPM), Dhahran, Saudi Arabia

ABSTRACT: Shape Memory Alloy (SMA) is a smart and intelligent material having potential for application as reinforcing steel in reinforced concrete smart structures. Superelastic SMAs have a unique ability to undergo large deformations under applied load, returning to a predetermined shape upon unloading. SMAs have a relatively lower modulus of elasticity and smaller hysteretic loop compared to that of steel. This unique property of SMAs makes it amenable to be used as reinforcement in RC elements for enhancing its ductility during seismic events. Several experimental investigations have been conducted in the recent years using SMA bars and wires in RC elements. This paper presents a finite element simulations of reinforced concrete (RC) flexural beam reinforced with superelastic SMA bars under cyclic loadings and the results are compared with the experimental data obtained from the tests condcuted at University of Illinois. The inelastic behavior of SMA bars in the cyclic load test of beam is captured by finite element simulations. The cracking load, initiation of flexural and shear cracks, forward, and reverse transformation, and mode of failure shows good agreement with the experimental data. The FE simulations shows that SMA bars have the ability of re-centering the beam, and can be used in RC beams to reduce permanent deformation leading to the closure of cracks in concrete.

## 1 INTRODUCTION

In a major seismic event, the response of reinforced concrete (RC) structures is characterized by failure of joints, shearing of columns and formation of hinges in beams, which leads to partial or complete collapse of these structures. The primary goal of all design codes is to protect the life and preclude the collapse of RC structures under seismic load. Reinforcing steel used in concrete structures has the ability to undergo large deformation under seismic loads causing permanent deformation in structural members through the well-defined hinges. The primary goals may be achieved but the serviceability of the structure could be lost due to large deformation, prohibiting the post-earthquake repair of the structures. One of the areas in seismic research is to develop new reinforcing material that has the ability to undergo large deformation with no permanent straining and resulting in repairable damage to the structure. A new material made from superelastic shape memory alloy (SMA) has emerged recently in the field of civil

engineering that can be used as reinforcement in concrete structures. SMAs have the ability to sustain large deformations under applied load and returns to its original shape after the removal load. Superelastic SMAs possess several properties that make them unique and desirable for use in concrete structures in a seismic region. SMA properties include recentering capabilities, hysteretic behavior and strain hardening under large deformation. Nickel-Titanium (NiTi) SMAs, consisting of nickel 56% and 44 % titanium alloy is the commonly investigated SMA for civil engineering applications.

A number of studies have been carried out on the material characterization and mechanical properties of SMAs. DesRoches et al. (2004) evaluated the superelastic properties of NiTi SMA wires and bars under cyclic loading. They reported that recentering capability is not affected by the size, but wire experiences high damping potential and strength than the SMA bars. The re-centering capabilities and damping increases by reducing the diameter of bar was also reported by McCormick et al. (2007). Zafar and Andrawes (2013, 2014) fabricated highly ductile superelastic SMA composites (100 % SMA wires and hybrid fibers of SMA and glass-FRP) and studied the cyclic behavior of composites. They also reported that SMA composite bars showed high ductility, recentering capabilities and energy dissipation as compared to the conventional FRP reinforcing bars. The SMA composite reinforcement used in RC beam enhanced the performance of member by re-centering and crack closing ability. Nehdi et al. (2009, 2011) studied the concrete beam-column joint with SMA bars and compared the results with conventional RC beam-column joint. It was observed that SMA beam-column joint showed sufficient energy dissipation under cyclic loading. Concrete cylinders confined using SMAs spirals showed significantly higher ultimate strain and strength as compared to conventional GFRP confined concrete cylinders (Shin et al., 2010). The behavior of superelastic SMA reinforced flexure-critical RC beams was investigated by Abdulridha et al. (2013). They reported that the SMA beams could recover large inelastic displacement after the removal of loads.

Several studies have been conducted recently focusing on the experimental investigations with SMA bars or wires in concrete structural elements. Very limited work has been done on numerical simulation of SMA reinforced concrete members using FEM approach. The main objective of this paper is to use the FEM method to investigate SMA reinforced RC member in flexure. Nonlinear finite element analysis is carried out to simulate the tests conducted on superelastic SMA reinforced concrete beam by Zafar and Andrawes (2013). Non-linear finite element analysis is carried out using the commercial finite element software ANSYS (ANSYS 12.1, 2009). The nonlinear SMA material model was adopted and loading and unloading cycles as reported in experimental program was applied to investigate the numerical response.

## 2 NON LINEAR FE ANALYSIS OF SMA REINFORCED BEAM

### *2.1 Experimental Beam Details*

The experimental beam studied by Zafar and Andrawes (2013) under cyclic loading is shown in Figure 1. Two SMA bars were used in T-beam without any stirrups. The projection at the ends was used for anchoring the rebar.

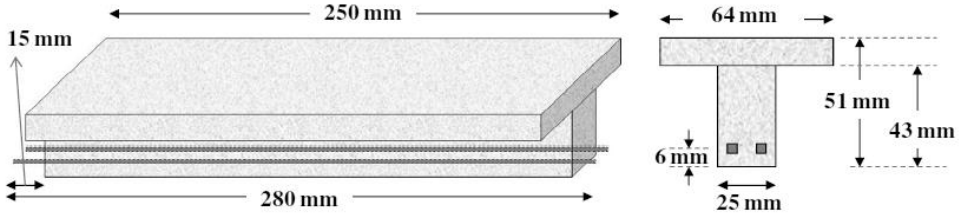


Figure 1. Cross sectional dimensions of T-beam tested (Zafar and Andrawes (2013))

The simply supported beam was tested in flexural by three-point bending test method. A notch was provided at the mid span to promote the crack at predefined location. The loading setup and support conditions are shown in figure 2.

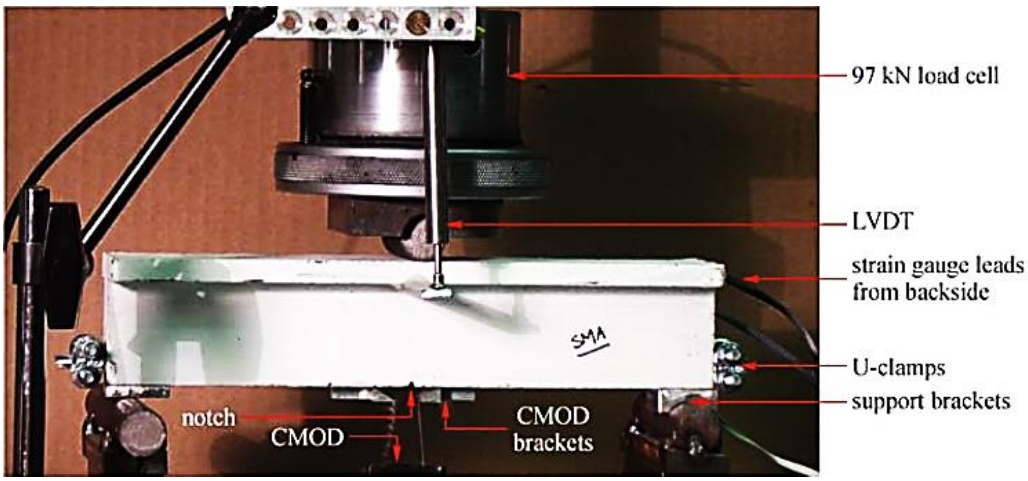


Figure 2. Experimental loading setup and support conditions (Zafar and Andrawes (2013))

### *2.2 ANSYS finite element model for SMA Reinforced Beam*

#### 2.2.1 Concrete model

Due to the symmetry in cross-section and loading half beam was modeled. The concrete was modeled using Solid65 element in ANSYS and the five-parameter Willam-Warnke material model for concrete (Willam and Warnke, 1975). This material model predicts the failure of concrete based on cracking and crushing failure modes. The criterion for failure of concrete due to a multiaxial stress state can be expressed in the form,

$$\frac{F}{f_c} - S \geq 0 \tag{1}$$

where; F: a function of the principal stress state ($\sigma_{xp}$, $\sigma_{yp}$, $\sigma_{zp}$)

S: failure surface expressed in terms of principal stresses and five input parameters $f_t$, $f_c$, $f_{cb}$, $f_1$ and $f_2$.

In addition, $f_t$ is the ultimate uniaxial tensile strength, $f_c$ is the ultimate uniaxial compressive strength, $f_{cb}$ is the ultimate biaxial compressive strength, $f_1$ is the ultimate compressive strength for state of biaxial compression superimposed on hydrostatic stress state and $f_2$ is the ultimate

compressive strength for state of uniaxial compression superimposed on hydrostatic stress state.

If equation 1 is satisfied, the material will crack or crush. The failure surface can be specified with a minimum of two constants, $f_t$ and $f_c$. The other three constants are calculated in the Willam-Warnke model by default as $f_{cb} = 1.2f_c$, $f_1 = 1.45f_c$ and $f_2 = 1.725f_c$. However, these default values are valid only for stress states where the hydrostatic stress state $|\sigma_h| \leq \sqrt{3} f_c$.

For finite element simulation, the compressive strength ($f_c$), tensile strength ($f_t$) and the modulus of elasticity ($E_c$) of concrete was taken as 55 MPa, 4.60 MPa and 34,856 MPa respectively.

### 2.2.2 SMA Model

Shape memory alloy was modeled using Solid185 element. The material model developed by Auricchio and Lubliner (1997) for SMA, which is available in ANSYS (2009) library was used for modeling the behavior of SMA bars in the beam. This material model has the ability to capture the behavior of superelastic SMA. The idealized stress-strain curve for SMA is shown in Figure 3.

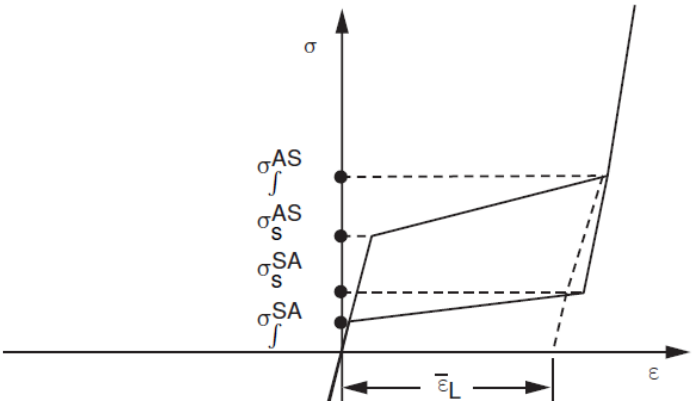


Figure 3. Idealized stress-strain diagram of superelastic SMA ANSYS

Where $\sigma_s^{AS}$ and $\sigma_f^{AS}$ are starting and final stresses for the forward transformation (Austenite to Martensite) respectively, $\sigma_s^{SA}$ and $\sigma_f^{SA}$ are starting and final stresses for the reverse transformation (Martensite to Austenite) respectively, and $\bar{\varepsilon}_L$ is the maximum residual phase. It is assumed that bars are perfectly bonded with concrete.

### 2.2.3 Steel Modeling

Steel plates were modeled using Solid45 element. Linear isotropic material modeled was used for steel plates with a modulus of elasticity for the steel. Figure 4 shows the beam model modeled in ANSYS (2009).

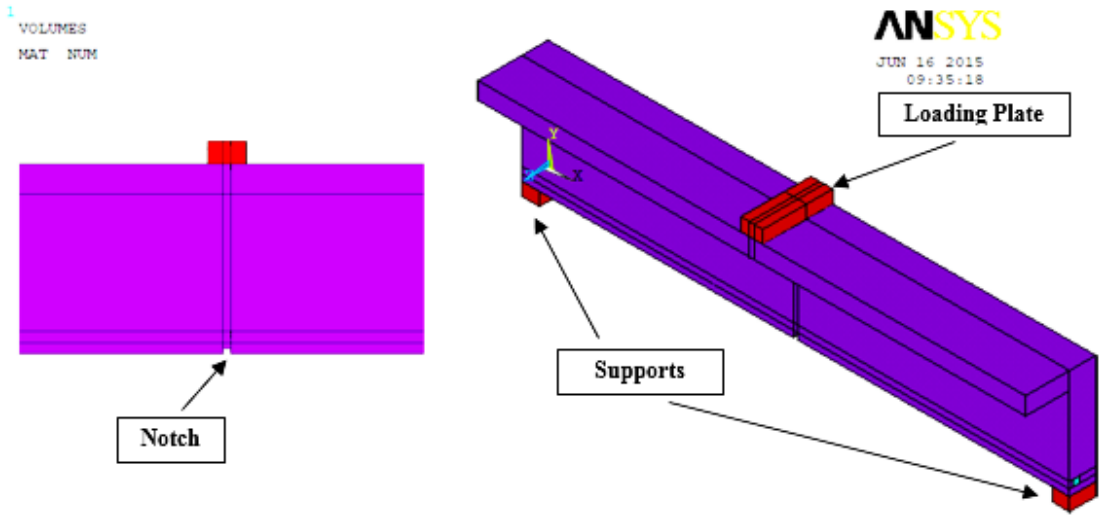


Figure 4. Finite element model of the SMA reinforced T-Beam in ANSYS

### 2.2.4 Loading and boundary conditions

The load was applied at the mid-span with repeated loading and unloading cycles. To get unique solution boundary conditions must be constrained. To confirm that model behaves similar to experimental beam boundary conditions were applied at the line of symmetry and supports. To initiate crack at pre-defined location the notch in the beam was also modeled. Figure 5 shows the boundary conditions, and the load applied in ANSYS (2009).

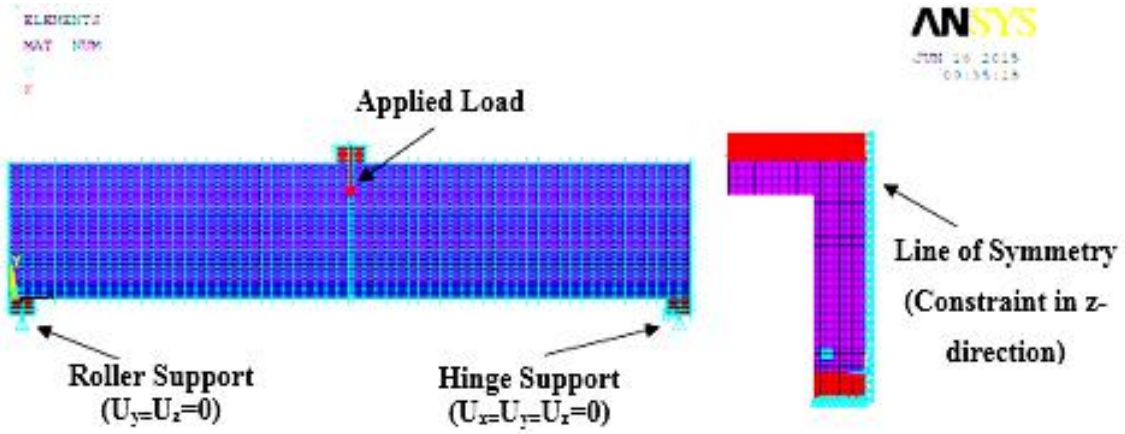


Figure 5. Boundary conditions and load applied

## 3 RESULTS AND DISCUSSIONS

The finite element simulations were carried out with the repeated loading and unloading cycles. In the first cycle beam was loaded up to Austenite phase (elastic range). Figure 6 shows the load-deflection curves of FE simulations and experimental results for 1$^{st}$ cycle. The first flexural crack in FE model was initiated at the notch at a cracking load of 1.309 kN with a corresponding deflection of 0.314 mm. In the experiment, the first flexural crack was reported at load of 1.31 kN with deflection of 0.29 mm. The first shear crack in FE model was observed at a

load of 2.50 kN with a deflection of 0.99 mm whereas, it was observed at a load of 2.63 kN with a corresponding deflection of 0.93 mm in the experiment. The loading phase for 1st cycle was completed at peak load of 3.05 kN with a deflection of 1.48 mm. Thereafter, the load was reduced until it reaches zero. When the beam was unloaded after first cycle, there was a 99.96% deflection recovery in the FE simulation (0.0005 mm), with no permanent deformation. However, during the actual experiment there was residual deflection of 0.57 mm, which can be attributed to the slippage of the SMA bars. Zafar and Andrawes (2013) reported that this slippage was observed due to the absence of dowel action, aggregate interlocking (because high strength grout was used instead of regular concrete) and smooth plain SMA bars.

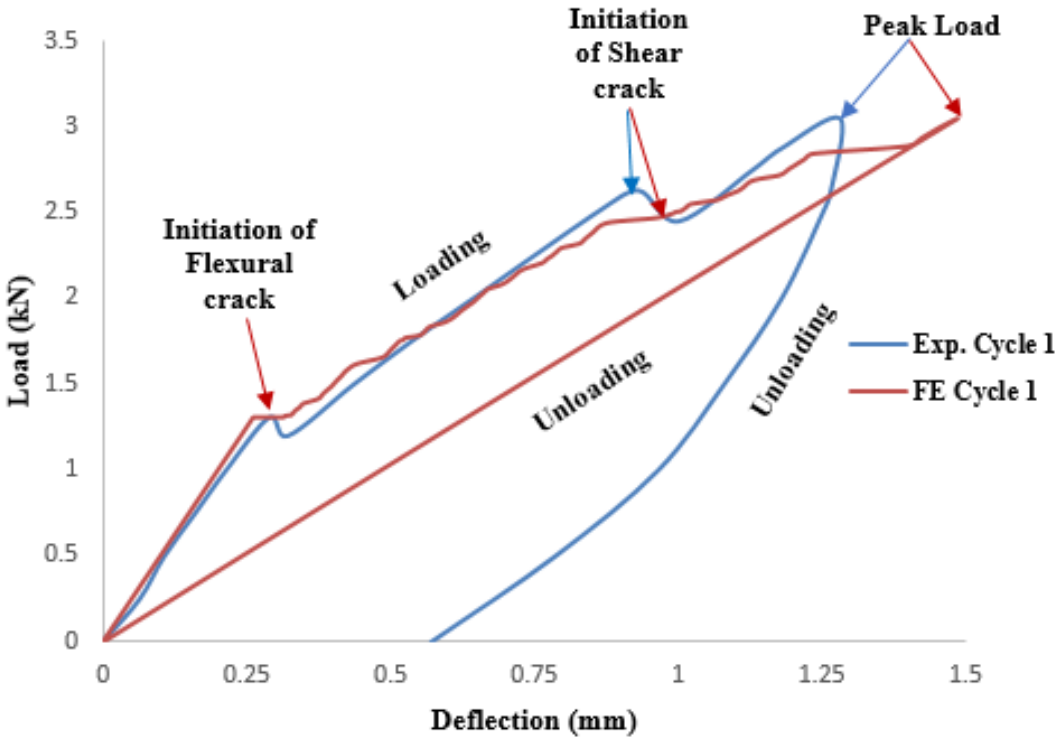


Figure 6. Load versus deflection between FE simulations and experimental for 1st cycle

In the 2nd cycle, the beam was loaded up to forward transformation. The load-deflection curves of FE simulations and experimental results for 2nd cycle is shown in Figure 7. The phase transformation from Austenite to Martensite (yielding of SMA) was observed at load of 3.56 kN with a deflection of 1.85 mm in FE simulations whereas, it was reported at load of 3.69 kN with deflection of 1.96 mm in the experiment. The loading phase of 2nd cycle was completed at load of 3.84 kN with deflection of 2.35 mm. At this point more flexural and shear cracks were observed in FE model. After unloading in the second cycle, the deflection in FE model was 0.00148 mm recovering 99.93 % deflection, whereas, during experiment deflection was recovered by 75 %. This indicates the re-centering of T-beam due to the presence of SMA bars.

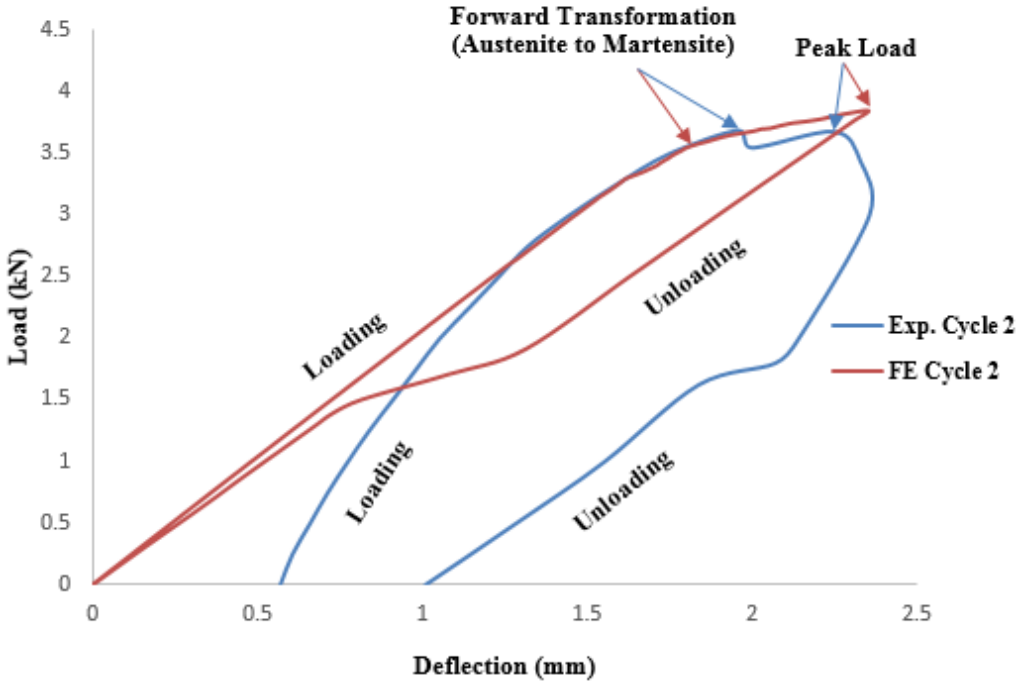


Figure 7. Load versus deflection between FE simulations and experimental for 2nd cycle

In 3rd cycle the beam was loaded up to the reverse transformation phase. Figure 8 shows the load-deflection curves of FE simulations and experimental results for 3rd cycle. The beam was loaded up to a load of 4.02 kN with a corresponding deflection of 3.36 mm. The reverse transformation (Martensite to Austenite start) and phase transformation (Martensite to Austenite finish) were observed at a load of 2.69 kN with a deflection of 2.37 mm and 1.50 kN with deflection of 0.78 mm, respectively. In experimental results, the reverse transformation (Martensite to Austenite start) and phase transformation (Martensite to Austenite finish) were reported at a load of 1.89 kN with a deflection of 2.92 mm, and 1.58 kN with a deflection of 1.98 mm, respectively. On unloading, the deflection in FE model was 0.0027 mm recovering 99.91 % deflection whereas, during the experiment, the deflection was recovered by 78 %. Almost complete recovery of deflection in FE simulation of beam is attributed to perfect bonding between SMA bars and concrete, whereas, in actual experiment bond slippage was observed and reported.

After the 3rd cycle, the beam was loaded until the solution stopped to converge, and at this stage, the complete shear failure was observed, which matches closely with the experimental data. The FE results give an insight into the behavior and the development of cracks in the beam reinforced with SMA bars. Figure 9 shows the flexural crack, which developed during 1st cycle in the load test on beam, which was also captured in the finite element simulation. Figure 10 shows, the initiation of shear crack and opening of flexural crack in the 1st cycle in the experimental beam and the FE simulation. The cracks continue to grow in width and number in the 2nd and 3rd cycles until shear failure of the beam at the final stage. Figure 11 shows the complete shear failure in the beam at the final stage in the actual beam, which was also captured in the FE simulation. The details of loads and deflection at various loading and unloading stages in the load test of the SMA reinforced beam and the ANSYS finite element simulation is shown in Table 1.

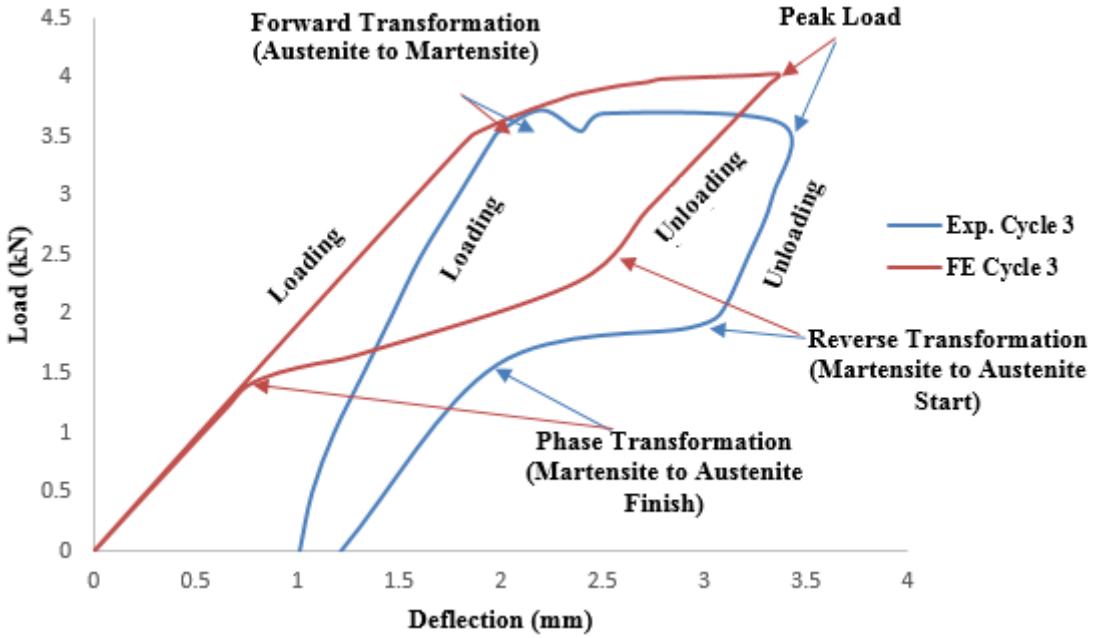


Figure 8. Load versus deflection between FE simulations and experimental for 3rd cycle

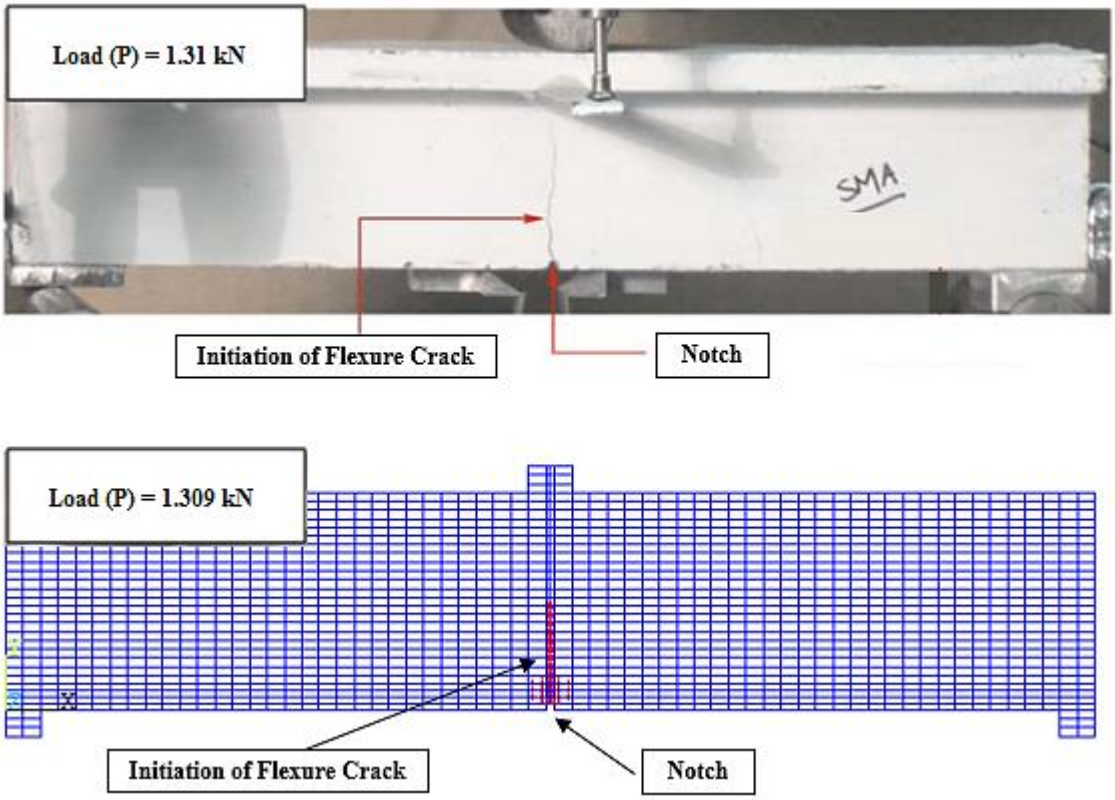


Figure 9. Initiation of flexural crack in the experimental and FE Simulation during 1st cycle

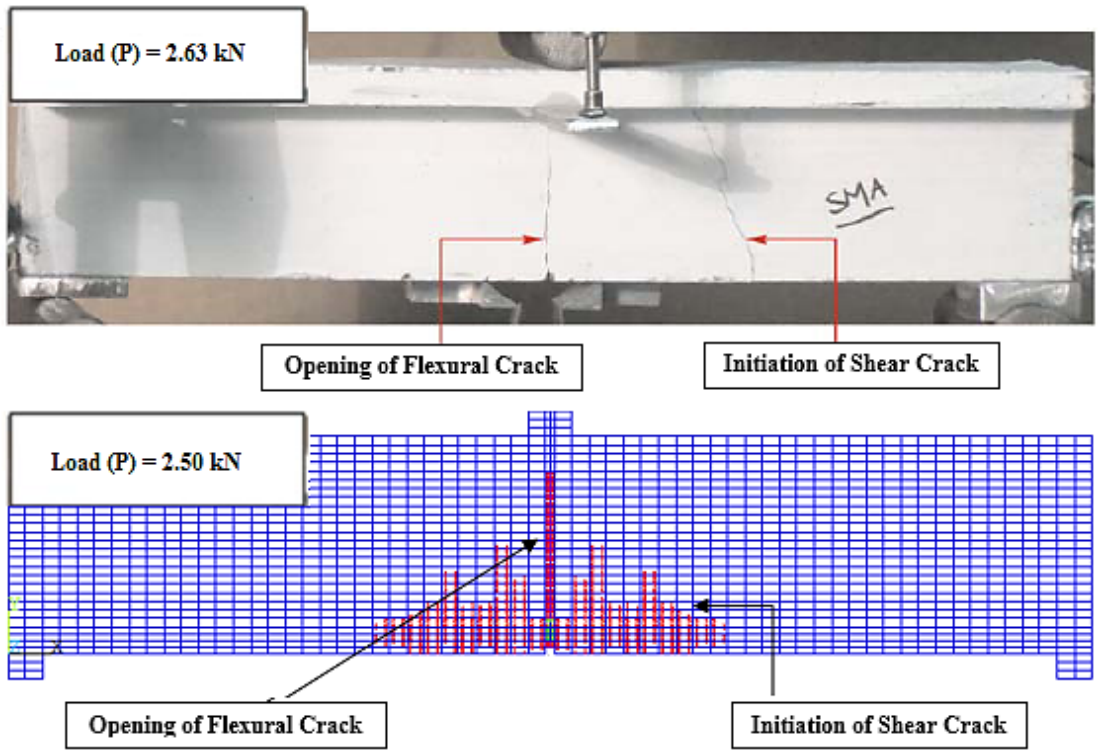


Figure 10. Initiation of shear crack in the experimental and FE simulation during 1st cycle

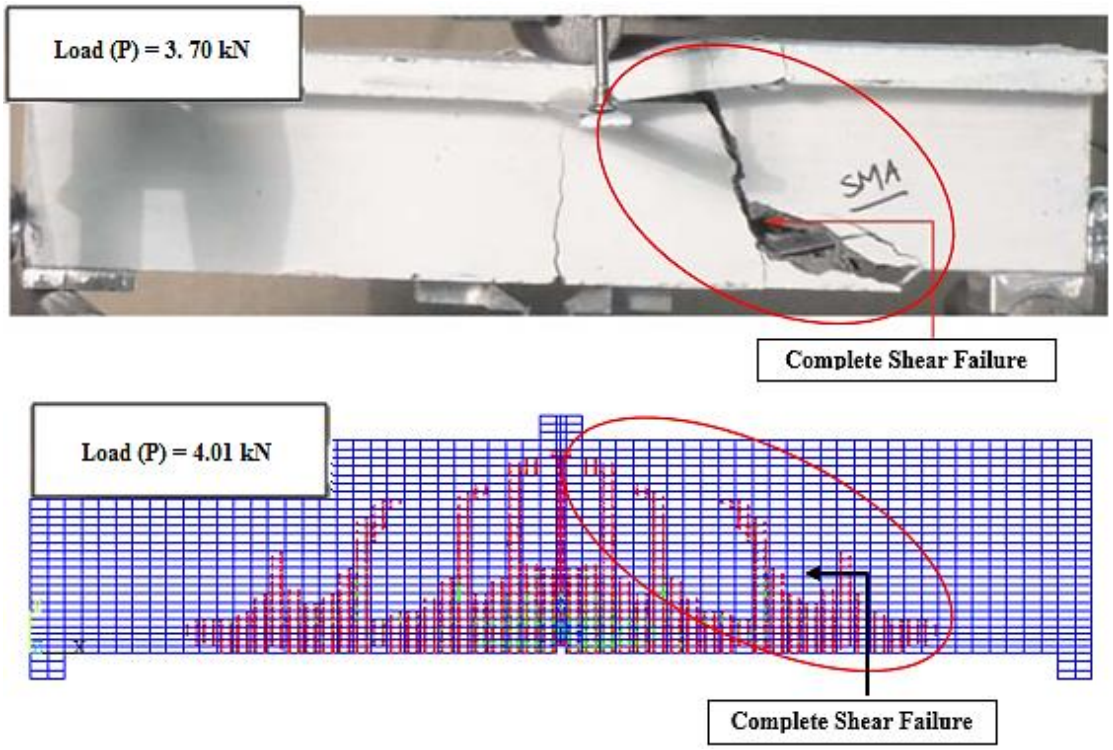


Figure 11. Complete Shear Failure in experimental and FE simulation at final stage

Table 1. Comparison of experimental and FE simulations

| Cycle | Phase | Description | Experimental | | FE Simulations (ANSYS) | |
|---|---|---|---|---|---|---|
| | | | Load (kN) | Deflection (mm) | Load (kN) | Deflection (mm) |
| 1 | Loading | Flexural crack initiation | 1.31 | 0.29 | 1.309 | 0.314 |
| | | Shear crack initiation | 2.63 | 0.93 | 2.5 | 0.99 |
| | | Maximum load for Cycle 1 | 3.05 | 1.28 | 3.05 | 1.48 |
| | Unloading | 1st Cycle End | 0 | 0.57 | 0 | 0.0005 |
| 2 | Loading | Forward Transformation (Austenite to Martensite) | 3.69 | 1.96 | 3.56 | 1.85 |
| | | Maximum load for Cycle 2 | 3.44 | 2.33 | 3.84 | 2.35 |
| | Unloading | 2nd Cycle End | 0 | 1.01 | 0 | 0.00148 |
| 3 | Loading | Forward Transformation (Austenite to Martensite) | 3.55 | 1.99 | 3.58 | 1.94 |
| | | Maximum load for Cycle 3 | 3.62 | 3.37 | 4.02 | 3.36 |
| | | Reverse Transformation (Martensite to Austenite Start) | 1.89 | 2.92 | 2.69 | 2.37 |
| | Unloading | Phase Transformation (Martensite to Austenite Finish) | 1.58 | 1.98 | 1.5 | 0.78 |
| | | 3rd Cycle End | 0 | 1.21 | 0 | 0.0027 |

## 4 CONCLUSIONS

Finite Element Simulation of a beam reinforced in flexure by SMA bars was carried out using ANSYS commercial software. Experimental investigation on SMA bar reinforced beam under cyclic loading was carried out by Zafar and Andrawes. The experimental response of the SMA reinforced beam was captured with a good accuracy using the SMA material model developed by Auricchio and Lubliner and the five-parameter Willam-Warnke model for concrete plasticity. A perfect bonding between SMA bars and concrete was assumed in the simulation. In the actual experiment, slip occurs between the SMA bars and the concrete (high strength grout beam) in the beam, which is attributed by the investigators to the absence of dowel action and aggregate interlocking. The slip was not captured due to perfectly bonded SMA bars in the finite element simulations. The response of the SMA reinforced beam, including the initiation of flexural and shear cracks, growth of flexural and shear cracks, transformation from Austenite to Martensite, reverse transformation in various cycles and the ultimate loads were predicted with a good accuracy. The final mode of failure was complete shear failure in experimental beam, which was also captured by FE simulation in ANSYS.

## 5 ACKNOWLEDGMENTS

This Research was funded by Deanship of Scientific Research, King Fahd University of Petroleum & Minerals under Project Number IN121058 titled "Investigation on efficacy of shape Memory alloys (SMAs) for strengthening and retrofitting of Beam-Column Joints (BCJs)", which is gratefully acknowledged. The support provided by the Department of Civil and Environmental Engineering and the Center for Engineering Research,Research Institute at KFUPM is also acknowledged.

## 6 REFERENCES

ANSYS 12.1 (2009), Finite element analysis system, SAS IP, Inc.

Auricchio, F. and Lubliner, J. (1997), Uniaxial model for shape-memory alloys, *International Journal of Solids and Structures*, 34: 3601-3618.

Auricchio, F., Taylor, R.F., and Lubliner, J. (1997), Shape-memory alloys: macromodeling and numerical simulations of the superelastic behavior, *Computational Methods in Applied Mechanical Engineering*, Vol. 146. pp. 281–312.

DesRoches, R., McCormick, J., and Delemont, M. (2004), Cyclic properties of superelastic shape memory alloy wires and bars, *Journal of Structure Engineering*, 130: 38–46.

Nehdi M., Alam M, Youssef M. (2011), Seismic behavior of repaired superelastic shape memory alloy reinforced concrete beam-column joint, *Smart Structure and System*, 7(5): 329-348.

Nehdi, M., Alam, M. S., and Youssef, M. A. (2009), Development of corrosion-free concrete beam column joint with adequate seismic energy dissipation, *Engineering Structure*, 32(9): 2518–2528.

Shin, M., and Andrawes, B. (2010), Experimental investigation of actively confined concrete using shape memory alloys, *Engineering Structure*, 32(3): 656–664.

Willam K. J. and Warnke E. D. (1975), Constitutive model for the triaxial behavior of concrete, Bergamo, Italy, *Proceedings, International Association for Bridge and Structural Engineering*, 19, 1-30.

Zafar A. and Andrawes B. (2013), Experimental flexural behavior of SMA-FRP reinforced concrete beam, Frontiers *of Structural and Civil Engineering*, 7(4): 341–355.

Zafar A. and Andrawes B. (2014), Fabrication and cyclic behavior of highly ductile superelastic shape memory composites, *Journal of Materials in Civil Engineering*, 26: 622-632.